Brain Areas Involved in Perception of Biological Motion

E. Grossman, M. Donnelly, R. Price, D. Pickens, V. Morgan, G. Neighbor, and R. Blake
Vanderbilt University

Abstract

■ These experiments use functional magnetic resonance imaging (fMRI) to reveal neural activity uniquely associated with perception of biological motion. We isolated brain areas activated during the viewing of point-light figures, then compared those areas to regions known to be involved in coherent-motion perception and kinetic-boundary perception. Coherent motion activated a region matching previous reports of human MT/MST complex located on the temporo-parieto-occipital junction. Kinetic boundaries activated a region posterior and adjacent to human MT previously identified as the kinetic-occipital (KO) region or the lateral-occipital (LO) complex. The pattern of activation during viewing of biological motion was located within a small region on the ventral bank of the occipital extent of the superior-temporal sulcus (STS). This region is located lateral and anterior to human MT/MST, and anterior to KO. Among our observers, we localized this region more frequently in the right hemisphere than in the left. This was true regardless of whether the point-light figures were presented in the right or left hemifield. A small region in the medial cerebellum was also active when observers viewed biological-motion sequences. Consistent with earlier neuroimaging and single-unit studies, this pattern of results points to the existence of neural mechanisms specialized for analysis of the kinematics defining biological motion. ■

INTRODUCTION

We live in a dynamic visual world: Objects often move about in our environment and we, as observers, are often moving as we look at those events. One of the most biologically salient events is, in fact, human movement. People are remarkably adept at recognizing the actions performed by others, even when the kinematic patterns of their movements are portrayed by nothing more than a handful of light points attached to the head and major joints of the body (Johannson, 1973). Individual, static frames look like meaningless clusters of dots, but when the frames are animated, one immediately perceives a biological organism engaged in a readily identifiable activity. With no more than 12 point-lights portraying biological motion, people can reliably discriminate male from female actors, friends from strangers (Cutting & Kozlowski, 1977), and even subtle differences in complex activities such as serving a tennis ball (Pollick, Fidopiastis, & Braden, 1999). Perception of biological motion is also robust to variations in the number of dots used and variations in exposure duration (Neri, Morrone, & Burr, 1998). Despite its robustness, perception of biological motion is severely degraded simply by inverting the animation sequences, thereby portraying the activity upside-down (Ahlstrom, Blake, & Ahlstrom, 1997; Sumi, 1984).

Of course, motion information is important for more than just identification of biological motion. Humans are adept at detecting weak coherent motion amidst a background of incoherent motion (Raymond, 1994; van de Grind, Koenderink, van Doorn, Milders, & Voerman, 1993; Williams & Sekuler, 1984; but see Barlow & Tripathy, 1997), are very accurate at judging the direction in which objects are moving (Gros, Blake, & Hiris, 1998; De Bruyn & Orban, 1988; Pasternak & Merigan, 1984; Ball & Sekuler, 1982), and, under optimal conditions, are keenly sensitive to slight differences in the speed at which objects are moving (Chen, Bedell, & Frishman, 1998; McKee & Welch, 1989; De Bruyn & Orban, 1988; Orban, De Wolf, & Maes, 1984). In addition, motion provides a potent source of information for specifying the 3-D shapes of objects (Tittle & Perotti, 1998; Sperling, Landy, Dosher, & Perkins, 1989; Lappin & Fuqua, 1983; Rogers & Graham, 1979; Wallach & O'Connell, 1953).

Reflecting the importance of motion information in perception, the primate visual system devotes considerable neural machinery to the analysis of motion information. From single-cell studies, it is known that neurons specialized for registration of motion are found in multiple visual areas of the dorsal pathways projecting from area V1, through V5/MT and to higher visual areas within the parietal lobe (Andersen, 1997; Newsome, 1997). In

recent years, important advances have been made in relating activity of neurons in some of these areas (most notably, MT and MST) to visual registration of coherent-translating motion (e.g., Shadlen, Britten, Newsome, & Movshon, 1996), 3-D surface shape from motion parallax (e.g., Bradley, Chang, & Andersen, 1998; Xiao, Marcar, Raiguel, & Orban, 1997), and complex-optical flow associated with looming and rotation (Lagae, Maes, Xiao, Raiguel, & Orban, 1994; Duffy & Wurtz, 1991; Saito et al., 1986). However, neurons in these visual areas do not seem particularly well-suited for the extraction of the complex kinematics characterizing biological motion. Are there other, more specialized areas where this processing might be accomplished? Single-unit recordings in the superior-temporal-polysensory area (STPa) of macaque monkeys have identified cells that respond selectively to biological motions, including some portrayed by point-light animations (Oram & Perrett, 1994). The STPa, incidentally, receives input from both the dorsal and ventral pathways, which is befitting the multidimensional nature of biological creatures engaged in diverse activities.

Is there evidence for the existence of neural mechanisms in the human brain specialized for the analysis of biological motion? Several lines of evidence point to an affirmative answer. Schenk and Zihl (1997a, 1997b) have described two patients with normal sensitivity to weak, coherent motion but with impaired ability to detect biological-motion figures portrayed against a background of static noise. On the other hand, the well-known patient, L.M., suffers impaired-speed-discrimination and elevated-coherence-detection thresholds, yet she experiences no difficulty recognizing and describing human activities portrayed by point-light displays (Vaina, Lemay, Bienfang, Choi, & Nakayama, 1990). These dissociated deficits imply that the neural mechanisms involved in detection of simple-translational motion differ anatomically from those underlying perception of biological motion.

Several recent neuroimaging studies also point to the existence of a region in the human brain uniquely activated by biological motion (perhaps the analog to the macaque STPa). Using functional magnetic resonance imaging (fMRI), Puce, Allison, Bentin, Gore, and McCarthy (1998) isolated a region in the right-posterior-superior-temporal sulcus (STS) that was activated when people viewed animation sequences showing eye and mouth movements. Using positron emission tomography (PET), Bonda, Petrides, Ostry, and Evans (1996) found that this same general region was activated when observers viewed point-light figures. Also using fMRI, Howard et al. (1996) found bilateral activation on the superior-temporal gyrus anterior to MT in response to viewing point-light animations. These investigators also found different patterns of activation within the MT/MST complex during observation of biological motion, optic flow, and coherent motion.

While these three studies agree that biological-motion perception may be linked to activity within a region near the posterior STS, it is questionable from those results whether this is the only neural area uniquely involved in seeing biological motion. In addition, it remained to be learned where this putative area exists relative to areas activated by other, non-biological animation sequences. The present experiments sought to address these remaining issues using fMRI. Specifically, we compared visual areas activated by biological motion to brain loci responsive to coherent motion, a stimulus known to activate the MT/MST complex (Cheng, Fujita, Kanno, Miura, & Tanaka, 1995; Tootell et al., 1995; Dupont, Orban, De Bruyn, Verbruggen, & Mortelsman, 1994; Watson et al., 1993) and to motion-defined shapes, a class of stimuli that activates the kinetic-occipital (KO) region (Van Oostende, Sunaert, Van Hecke, Marchal, & Orban, 1997; Orban et al., 1995) or area LOC/LOP as it is called by some (Tootell, Hadjikhani, Mendola, Marrett, & Dale, 1998). The inclusion of motion-defined shapes in our study seemed particularly relevant given that biological motion has been characterized as a motion-contour-discrimination problem (Grossberg & Rudd, 1989).

RESULTS

Group Results

Averaging statistical maps for all seven observers in stereotaxic space revealed stimulus-specific clusters of activation. Here, we consider each of these clusters in turn.

The coherent-motion condition (coherent motion minus static dots) revealed bilateral clusters of intense activity within a sulcus between the lateral-occipital (LO) sulcus and the inferior-occipital sulcus, at the juncture of the temporal, parietal, and occipital lobes (see Figure 1B). Previous reports define this location as the MT/MST complex (Sunaert, Van Hecke, Marchal, & Orban, 1999; Tootell et al., 1995; Dupont et al., 1994; Watson et al., 1993). While activation was reliably bilateral, the precise location and extent differed slightly between the two hemispheres, with the right-hemisphere MT+ appearing slightly dorsal and medial relative to the left hemisphere. Others have reported more variability in the left-hemisphere MT+ across observers (Howard et al., 1996), and our results also show this tendency.

The kinetic-boundary minus coherent-motion condition revealed a large region of activation adjacent and posterior to the MT+, strongly correlated to the presence of kinetic contours (Figure 1C). This region was superior and anterior to MT/MST, located along the LO sulcus. Our kinetic-boundary stimulus is almost

Figure 1. Schematics of the various visual stimuli and the corresponding correlated neural activity. The actual stimuli were short animations of black dots on a gray background. Neural images reflect the group-averaged activation. (A) In the biological-motion condition, point-light figures were interleaved with scrambled motion. The biological-motion dots represented all the major joints and head of an actor performing some activity (in this case, a karate kick). Scrambled displays have all the same motion vectors as biological motion, but the initial starting positions were randomized so that any spatio-temporal relations among the dots were destroyed. The correlated activity averaged across all subjects revealed a single locus of activation on the posterior STS. (B) In the coherent-motion condition, animations of coherent motion were interleaved with static dots. Correlated activity revealed MT+, a region located between the LO and inferior-occipital sulci. (C) The kinetic-boundary animations were interleaved with coherent motion. The only difference between these two stimuli was the presence of illusory contours in the kinetic-boundary stimulus. The resulting neural activity was found posterior to MT+ and corresponds to previous reports of KO/LO. (D) 3-D rendering of group activation resulting from the coherent-static condition (blue), and the biological-scrambled condition (red). The overlap of the two areas is defined in green.

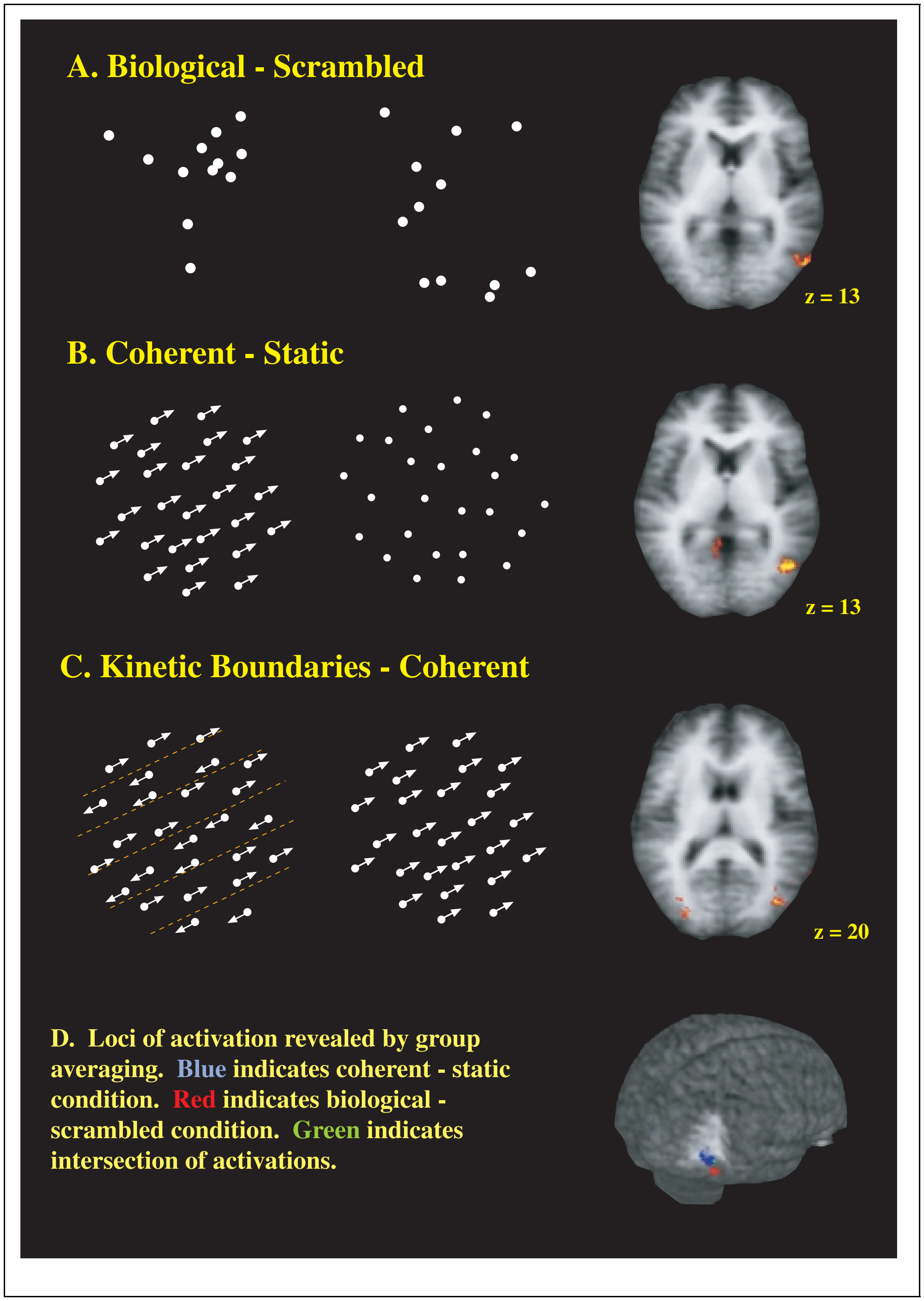

identical to that used by Van Oostende et al. (1997), and the activation we observed corresponds to the regions they localized. We assume, therefore, that this is the area specialized for processing kinetically defined contours, which the Belgium group has dubbed KO.

Neural activation during the biological-motion condition (biological motion minus scrambled motion) appeared in a region distinct from MT/MST and KO (Figure 1A). This locus of correlated activity was found along the ventral bank of posterior STS, just behind the dorsal bend. This region is on the same horizontal slice as MT+, but located more laterally (see Figure 1D). Again, activation was bilateral but, in the group average, it was more highly correlated and larger in extent in the right hemisphere.

Individual Results

Based on the group activity and the anatomy of the individuals, regions corresponding to MT+, KO, and

posterior STS were defined for each observer. For all seven observers (and therefore 14 hemispheres), we were able to identify highly correlated voxels corresponding to MT+ in every hemisphere (see Table 1). Only eight hemispheres had correlated voxels within the LO sulcus, corresponding to the KO area. Six of these eight KO regions were found in the right hemisphere. Eight regions of correlated activity were identified on the ventral bank of the posterior STS, five of which were in the right hemisphere.

The correlations between the activity profiles and the stimulus presentation for the three conditions were computed for each neural area of interest found in our observers (see Table 2 and Figure 2). Not surprisingly, in all three regions, activity was most highly correlated with the stimulus used to localize that region (this corresponds to the diagonal scores in Table 2). The activity of a given area during the other two stimulus conditions was not tightly correlated to the periodicity of the stimulus epochs. For example, posterior STS was reliably activated in the presence of biological motion, but was simply not activated by coherent motion, static dots, or kinetic contours.

This is not to say that biological motion did not activate MT+. In fact, activity levels in MT+ during the biological-motion condition initially rose and remained constant throughout the entire period of stimulation. However, this elevated activity did not change throughout the interleaved-biological and scrambled animations; MT+ does not differentiate between biological and scrambled stimuli. Likewise, MT+ is indiscriminately activated by kinetic boundaries and coherent motion.

Hemifield Inputs to Posterior STS

Having identified a region uniquely associated with viewing biological motion, we next studied the visual-field topography of this region. To accomplish this, we measured fMRI signals to biological and scrambled sequences presented either to the left or to the right of a central fixation point. Observers carefully maintained strict fixation, insuring that the animations were imaged in one visual hemifield only. In all other respects, data collection and analysis were identical to the procedures used in the main experiment.

Table 2. Average MR Signal Correlation to Stimulus Presentation Across Observers for MT+, KO, and Posterior STS. Correlations are Highest along the Diagonal, which were the Conditions Used to Localize Each Neural Area. Correlations Off the Diagonal Indicate Activity of the Area During the Other Stimulus Conditions. Parenthesis Indicate Standard Error

	Posterior STS	*MT+*	*KO/LO*
Bio-Scram	0.54 (0.11)	0.30 (0.20)	0.08 (0.16)
Coh-Static	0.25 (0.24)	0.64 (0.05)	0.13 (0.12)
Kin-Coh	−0.08 (0.21)	−0.17 (0.31)	0.51 (0.12)

In all four observers tested, we found reliable bilateral activation associated with both hemifield conditions (Figure 3). Activation of either hemisphere by biological motion is not dependent on whether the animation sequence appeared in the left- or the right-visual field. These findings demonstrate that the strict contralateral organization of visual field maps so diagnostic of early visual areas (e.g., Engel, Glover, & Wandell, 1997) gives way to bilateral representation within this higher visual area concerned with biological motion. This is not too surprising, given that single cells in parietal-lobe areas have receptive fields that extend well into the ipsilateral-visual field (Motter, Steinmetz, Duffy, & Mountcastle, 1987).

Cerebellar Involvement in Biological Motion

In one of our scanning sessions, we placed axial slices for one observer lower than we typically use. Consequently, those slices included portions of the cerebellum, and we were surprised to find high levels of activation in this structure produced by the biological-motion condition (biological minus scrambled). This serendipitous finding motivated us to measure fMRI activity at these slice planes in three other observers. Figure 4 shows the activation profile for a 26-voxel region of the cerebellum

Table 1. Number of Localized Regions (Out of a Possible Seven) in Each Hemisphere, and Center of Mass Coordinates in Talairach Space for Functionally Defined MT+, KO/LO, and Posterior STS. Coordinates Indicate the Group Mean for All Seven Observers and Parenthesis Indicate Standard Errors

	Right hemisphere				*Left hemisphere*			
	Num	*x*	*y*	*z*	*Num*	*x*	*y*	*z*
Posterior STS	5 (7)	−53.8 (4.3)	60 (4.3)	13 (9.9)	3 (7)	44 (7.8)	60 (5.5)	19 (9.3)
MT+	7 (7)	−48 (4.3)	61 (4.3)	10 (6.3)	7 (7)	43 (10.0)	61 (4.0)	14 (8)
KO/LO	6 (7)	−37 (9.4)	75 (5.2)	21 (12.1)	2 (7)	26 (3.5)	76 (2.1)	27 (2.1)

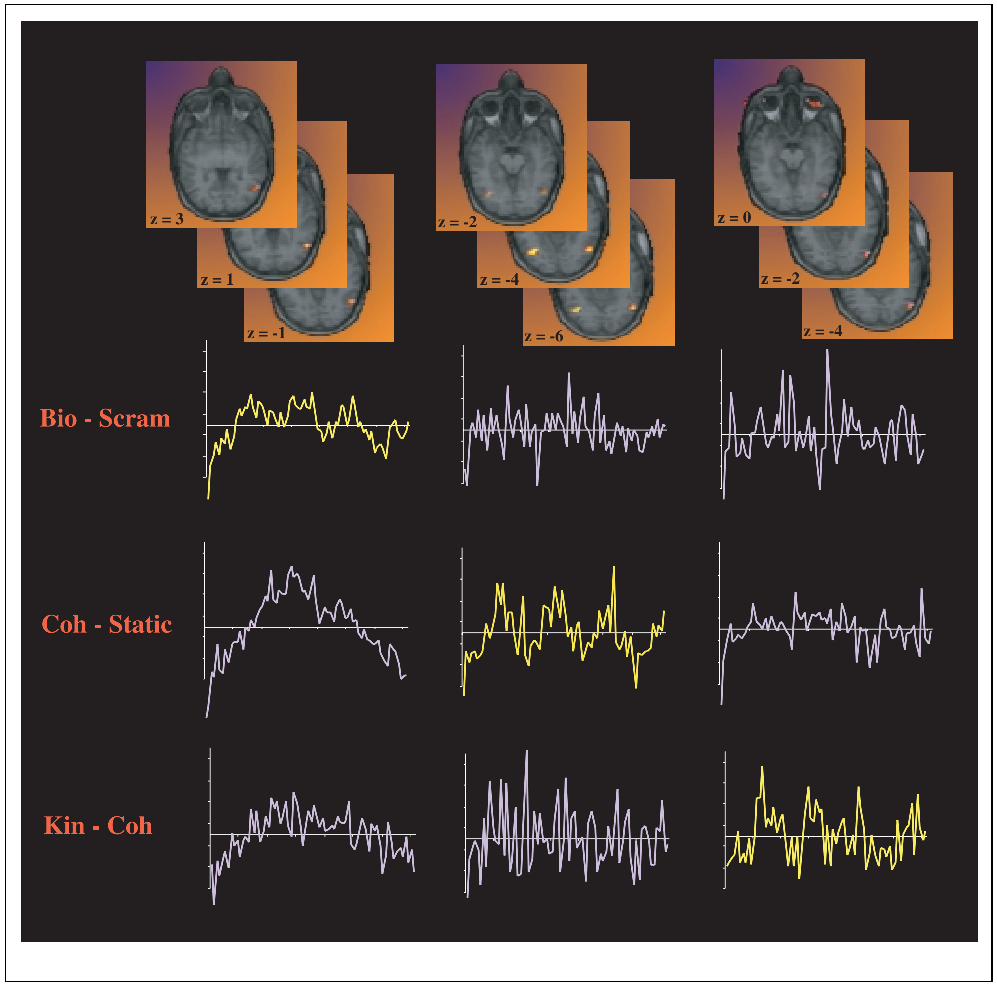

Figure 2. Activity profiles from a single observer (MF) for the three neural areas of interest during each stimulus condition (columns indicate neural area, rows indicate stimulus condition). Yellow time-series indicate the localizing condition (e.g., MT+ was localized using the coherent-static condition). Gray time-series indicate activity during the other stimulus conditions. Activity in each region is only highly correlated to stimulus periodicity during the localizing conditions.

for one observer during viewing of biological and scrambled motion. Here, it can be seen that viewing biological motion does indeed generate a signal in the anterior portion of the cerebellum, starting near the midline.

It is perhaps not so surprising that biological motion activates the cerebellum. For one thing, there is clinical evidence that the cerebellum is involved in motion perception. Specifically, patients with acute-cerebellar lesions are more variable on a task involving perception of apparent motion (Ivry & Diener, 1991) and are poorer at direction discrimination using coherent motion displays much like the ones used by us (Nawrot & Rizzo, 1995). These deficits are not simply the result of defective eye movements or unstable fixation, but, instead, imply that the cerebellum comprises part of the neural circuitry involved in motion perception (Gao et al., 1996). Besides its possible involvement in motion perception, the cerebellum also appears to be involved in cognitive tasks, including those which require judgments about motor activity (Fiez, 1996). So, for example, Petersen, Fox, Posner, Mintun, and Raichle (1989), found right-cerebellar activation when subjects were required to generate action verbs in response to visually presented nouns. Perhaps, then, observers in our experiments are unwittingly "labeling" the activity portrayed in biological-motion sequences, thereby producing activation through cognitive channels. It remains for future work to sort out the details of the

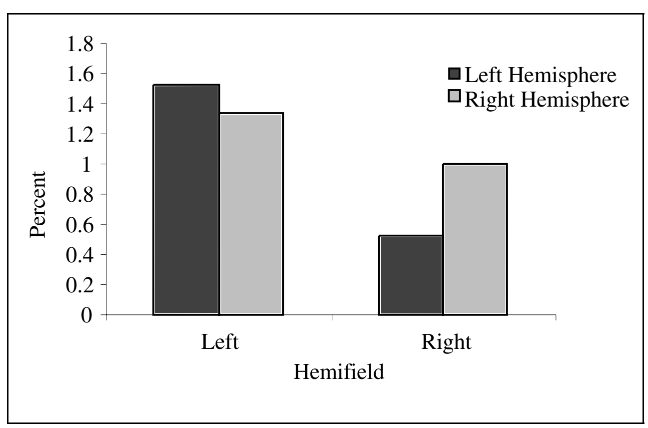

Figure 3. MR signal changes from right- and left-posterior STS during viewing of the point-light figures in each hemifield. Dark-gray bars indicate activity during stimulus presentation in the right hemifield. Light-gray bars indicate activity during presentation in the left hemifield.

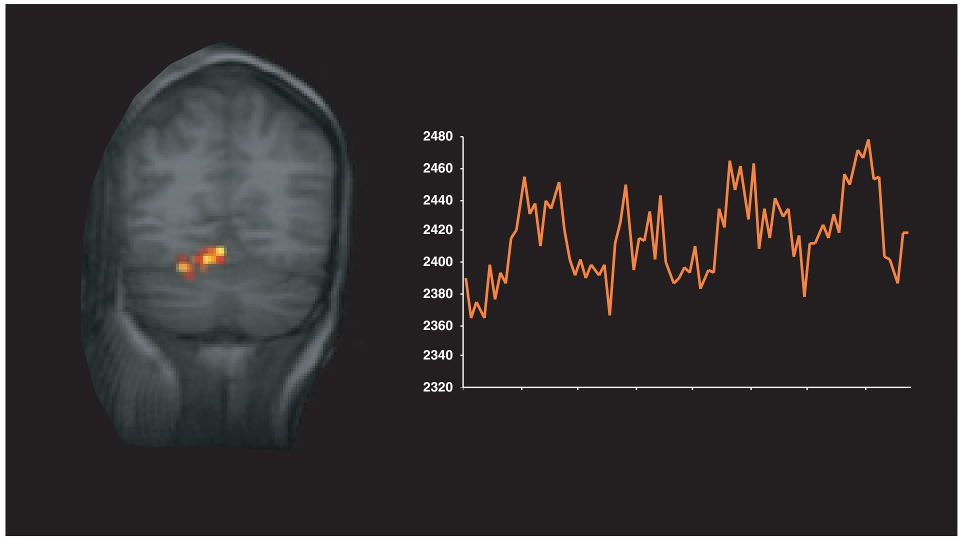

Figure 4. MR signal from a 26-voxel region in the cerebellum (individual observer) correlated to stimulus presentation during the biological-motion condition. This region of the cerebellum preferred biological motion over scrambled motion.

cerebellum's involvement in biological-motion perception.

DISCUSSION

Behavioral evidence from psychophysics (Neri et al., 1998), case studies in motion-impaired patients (Schenk & Zihl, 1997a, 1997b; Vaina et al., 1990), and single-unit recordings in monkeys (Oram & Perrett, 1994) all point to the existence of neural mechanisms specialized for registration of biological motion. Our results are consistent with other neural-imaging studies pinpointing that area to the STS in the human brain (Puce et al., 1998; Bonda et al., 1996). This small STS region is highly responsive when one views point-light sequences depicting biological motion, but it is neither activated by scrambled versions of those sequences, nor by coherent motion or kinetic boundaries.

While there is no indication that the MT+ complex was differentially active during the biological sequences, activity in this complex was certainly elevated at the onset of the biological-motion test sequences, and it remained high throughout the sequences. It seems reasonable to conclude, therefore, that this motion area provides at least some of the afferent signals innervating area STS. We stress ''feed-forward'' rather than ''feed-back'' signals, since activity in MT+ is not differentially modulated during presentation of the biological sequences.

It is interesting to note that the region we localized using whole-body motion is the same region Puce et al. (1998) found to be active during the viewing of mouth and eye movements. The common denominator in the two studies is the animate nature of the stimuli, not the particular kinds of motion being portrayed. In future works, it will be informative to learn just what aspects of the kinematic patterns associated with biological motion are necessary for activation of the posterior STS.

Finally, we are intrigued by the activation in the cerebellum associated with observation of biological motion. This finding is perhaps not so surprising, for there is good evidence for overlap between neural mechanisms involved in the planning of motor acts and mechanisms involved in perception of motor activities (e.g., Decety & Grezes, 1999). This encourages us to expand the survey of brain areas activated by biological motion to motor and premotor areas in the frontal lobes. With the spatial resolution of fMRI, it should be possible to differentiate activity, say, associated with the foot versus the hand. In addition, it remains to be seen whether brain areas activated by viewing biological motion can also be activated by motor imagery of those actions.

METHODS

Observers

Seven right-handed observers (four women, three men ranging in age from 24 to 52 years) with normal or corrected to normal vision participated in this experiment. All observers were informed of the possible risks associated with MR and gave informed consent as approved by the Vanderbilt University Institutional Review Board.

Procedure

Procedures were run in the Vanderbilt Medical Center on a 1.5-T GE Signa MR scanner with echospeed gradients. Each experimental session lasted approximately 1 hr. Animation sequences were back-pro-

jected onto a screen located at the observer's feet and viewed through a periscope mirror attached to the birdcage head coil. The periscope position was adjusted prior to each session to allow a full field of view outside the magnet bore. High-resolution anatomic images (T1-weighted, 60 sagittal slices, 2.5-mm thick with no gap, in-plane resolution 0.9375 mm, square pixels) were used to identify landmarks associated with the neural activity found in the functional images.

Observers participated in at least three functional runs, each designed to localize particular areas of interest. Axial slices (gradient-recalled echo-planar imaging, TR = 4000 msec, TE = 60 msec, flip angle = 90°, six slices, 5-mm thick, 1-mm gap, in-plane resolution 3.75 mm, square pixels) covered a 36-mm section of the brain including the majority of the occipital lobe, and the juncture of the occipital, temporal, and parietal lobes. Each functional run lasted 322 sec. The initial 32 sec of each run was a rest period during which the observer stared at a small cross located at the center of the screen. Following this rest period, two motion stimuli were presented in alternating 36-sec epochs.

During each stimulus epoch, observers viewed 16, 1-sec animation sequences, each separated by approximately 1 sec. Throughout each epoch, the observer performed a "one-back" task by tapping a finger whenever the same stimulus appeared on two (or more) successive presentations. Engaging the observer in a display-related task is particularly important given that attention can modulate neural response in visual areas (e.g., Watanabe et al., 1998). Although behavioral responses were not recorded during the actual scan session, all observers practiced the task before going into the magnet. The animation sequences used in the practice session were identical to those seen in the experimental conditions.

Stimuli

All animations consisted of dot cinematograms depicting three different kinds of motion events: coherent-translational motion, kinetic-boundary motion, and biological motion (Figure 1); multiple exemplars of each motion type were computer-generated off-line and replayed for presentation in the scanner. In all animations, the dots appeared black against a gray background (7 cd/m^2), and each dot subtended approximately 12 arc min. The duration of each animation exemplar was 1 sec. The interframe interval was dictated by the biological stimuli, which required three video retraces to produce the perception of smooth "biological" motion. The average speed within a sequence was about 4°/sec, a value within the optimal range for generating fMRI signals in motion areas of the human brain (Chawla et al., 1999). A fixation mark remained present in the center of the display for the duration of the functional run. Although we did not monitor eye movements, observers were instructed to maintain strict fixation throughout all stimulus conditions.

In the first functional condition (coherent motion), coherently moving dots were interleaved with static dots. The coherent-motion stimulus consisted of 100 dots moving at a constant velocity (4°/sec) within a 4.7° circular aperture. This dot speed approximated the average speed in the biological-motion sequences. Dot motions were wrapped such that dots moving out of the aperture were replaced on the other side of the window in the next frame. Direction of motion for a given 1-sec presentation was randomly chosen from a set of 24 values sampled in 15° intervals around the clock. The static dot array consisted of 100 dots imaged within the same 4.7° circular aperture. These dots were presented for 1 sec, followed by an 800-msec blank interval, which was set to approximate the interval between the motion stimuli.

In the second functional condition (kinetic boundary), kinetic-boundary exemplars were interleaved with presentations of coherent motion. Kinetic boundaries were created by dividing the 4.7° circular aperture into eight "strips" such that dots within adjacent strips moved in opposite directions. This display creates the impression of boundaries, or illusory contours, separating the opposing areas of motion. Like the coherent-motion display, the opposing directions of motion were sampled from intervals around the clock producing contours that varied over 24 different orientations. In all other respects, the kinetic-boundary sequences were identical to the coherent-motion stimuli.

In the third functional condition (biological motion), biological-motion animations were interleaved with sequences of scrambled motion. Biological motion was created by appropriate placement of 12 dots on the limbs and head of an actor engaged in various activities including jumping, kicking, running, and throwing (Ahlstrom et al., 1997). Scrambled versions of each sequence were created by randomizing the initial starting positions of the dots (constrained to approximate the dot density of the biological-motion figures) and leaving the motion paths intact. Thus, the scrambled sequences contained exactly the same individual-motion vectors as the biological displays, but with the coherent-spatial relations among dots destroyed. These scrambled movies resemble a cluster of dots moving at different speeds in various directions, with an overall motion "flow" in common (corresponding to the net flow of the biological sequence).

Image Analysis

A major purpose of our study was to identify and localize activation uniquely associated with viewing biological-motion sequences and to compare that to activation

associated with viewing coherent motion and kinetic boundaries. These latter two classes of displays have been used in several previous studies and, consequently, their unique activation is reasonably well-established. In overview, our analysis consisted of several steps: (i) Construct statistical maps of the correlation between the BOLD signals and stimulus timecourses for each observer, (ii) Transform each observer's activation map into a common coordinate system, (iii) Identify regions of significant activation from the averaged map, (iv) Based on anatomical landmarks in the group average, identify these regions-of-interest (ROI) in each observer, and (v) For each observer, compute the correlation of voxels in these ROI with the three types of motion displays. The following gives details of these steps.

Images were transferred from the scanner to a Silicon Graphics dual processor SGI Octane/SE for off-line analysis using AFNI 2.23 (Cox & Hyde, 1997). The first image of each sequence was used as the prototype to which all the subsequent images were aligned, correcting for both in-plane and out-of-plane motion. The first eight timepoints (32 sec) of each functional run were discarded to allow for stabilization of the MR signal. The first timepoint (4 sec) from each stimulus block was also discarded from the analysis to compensate for a hemodynamic lag. All image sequences were corrected for linear drift.

The remaining 64 timepoints for each voxel in every slice were cross-correlated with a boxplot defined by the stimulus on and off phases (minus the first 4 sec of each phase). The resulting statistical maps (R scores) for each observer were smoothed using a gaussian filter (7.5-mm FWHM) and then averaged with the original, unsmoothed statistical map (as described in Skudlarski, Constable, & Gore, 1999). This multifiltering technique minimizes small, single voxel sites of false-positive noise activation while emphasizing highly correlated clusters of activation.

The smoothed statistical maps of each observer were transformed to stereotaxic coordinates using a two-step algorithm applied to the high-resolution, whole-brain T1-weighted images. First, the origin was set on the midsagittal plane at the intersection of the dorsal and caudal edge of the anterior commissure. The rotational axis was defined between the ventral edge of the posterior commissure and the origin. The image was rotated to align the ac/pc axis, and then, second, the outermost boundaries of cortex were identified. The cortex was divided into 12 regions, and each region was linearly stretched or compressed to match the Talairach atlas (Talairach & Tournoux, 1988). The resulting transformation was then applied to the statistical maps of each observer, and these transformed maps were then averaged across observers to produce a single group-average map. Because the transformation from a unique observer space to a stereotaxic space is a relatively coarse one, identical anatomical landmarks in the brain often do not fall exactly within the same stereotaxic region in all observers. Spatially smoothing the statistical maps of each observer minimizes these individual differences.

The next step involved identifying regions of activation for each of the three stimulus conditions in the group-averaged map. Because averaged R scores are not a tabulated distribution, the Fisher–Cornish expansion (1960) was used to choose a threshold value corresponding to a voxel-wise $p < .001$. In setting the statistical threshold, we did not correct for multiple comparisons for three reasons. First, spatially smoothing the individual observers' maps guarantees lack of independence of neighboring voxels. Second, because each voxel in the group map is the average of seven independently sampled r scores (one from each observer), the probability of a false-positive occurring at the same location across multiple subjects is small. And third, the purpose of this group-average map was simply to focus our analyses of BOLD signal fluctuations on specific cortical areas of the individual observers.

The loci of activation found in the group map for each of the three stimulus conditions were identified in reference to specific anatomical landmarks and served as "masks" for identifying sites of activation within individual observers. Using a back-transformation from stereotaxic space to individual observer space, the masks were overlaid onto the T1-weighted anatomical images. Only those voxels within the masked regions that had activity correlated with the relevant task ($p < .05$, uncorrected) were included in the ROI and considered for further analysis. Again, we did not correct for multiple comparisons because the search for significance was constrained to regions identified in the group average, which constituted at most 25 voxels in each hemisphere (less than 1% of the total sampled voxels). The time-series from each voxel falling within an identified ROI was detrended, centered around zero by subtracting the mean, and averaged with all other voxels in that ROI. This step was repeated for each of the three stimulus conditions. The three resulting average time-series for each region were then cross-correlated with the boxplot defining the display conditions.

Acknowledgments

Supported by NIH EY07760, NIH EY01826, NIH EY07135, and the Discovery Program (Vanderbilt University). We thank Sang-Hun Lee and Stephen Rao for their helpful discussions.

Reprint requests should be sent to: Emily Grossman, Department of Psychology, Vanderbilt University, Nashville, TN 37240, e-mail: e.grossman@vanderbilt.edu.

REFERENCES

Ahlstrom, V., Blake, R., & Ahlstrom, U. (1997). Perception of biological motion. *Perception, 26,* 1539–1548.

Andersen, R. A. (1997). Neural mechanisms of visual motion perception in primates. *Neuron, 18,* 865–872.
Ball, K., & Sekuler, R. (1982). A specific and enduring improvement in visual motion discrimination. *Science, 2128,* 697–698.
Barlow, H., & Tripathy, S. P. (1997). Correspondence noise and signal pooling in the detection of coherent visual motion. *Journal of Neuroscience, 17,* 7954–7966.
Bonda, E., Petrides, M., Ostry, D., & Evans, A. (1996). Specific involvement of human parietal systems and the amygdala in the perception of biological motion. *Journal of Neuroscience, 16,* 3737–3744.
Bradley, D. C., Chang, G., & Andersen, R. A. (1998). Encoding of three-dimensional structure-from-motion by primate MT neurons. *Nature, 392,* 714–717.
Chawla, D., Buechel, C., Edwards, R., Howseman, A., Josephs, O., Ashburner, J., & Friston, K. J. (1999). Speed-dependent responses in V5: A replication study. *Neuroimage, 9,* 508–515.
Chen, Y., Bedell, H., & Frishman, L. J. (1998). The precision of velocity discrimination across spatial frequency. *Perception and Psychophysics, 60,* 1329–1336.
Cheng, K., Fujita, H., Kanno, I., Miura, S., & Tanaka, K. (1995). Human cortical regions activated by wide-field visual motion: an $H_2{}^{15}O$ PET study. *Journal of Neurophysiology, 74,* 413–427.
Cox, R. W., & Hyde, J. S. (1997). Software tools for analysis and visualization of FMRI Data. *NMR in Biomedicine, 10,* 171–178.
Cutting, J. E., & Kozlowski, L. T. (1977). Recognition of friends by their walk. *Bulletin of Psychonomic Society, 9,* 353–356.
De Bruyn, B., & Orban, G. A. (1988). Human velocity and direction discrimination measured with random dot patterns. *Vision Research, 28,* 1323–1335.
Decety, J., & Grezes, J. (1999). Neural mechanisms subserving the perception of human actions. *Trends in Cognitive Neuroscience, 3,* 172–178.
Duffy, C. J., & Wurtz, R. H. (1991). Sensitivity of MST neurons to optic flow stimuli. I. A continuum of response selectivity to large-field stimuli. *Journal of Neurophysiology, 65,* 1329–1345.
Dupont, P., Orban, G. A., De Bruyn, B., Verbruggen, A., & Mortelmans, L. (1994). Many areas in the human brain respond to visual motion. *Journal of Neurophysiology, 72,* 1420–1424.
Engel, S. A., Glover, G. H., & Wandell, B. A. (1997). Retinotopic organization in human visual cortex and the spatial precision of functional MRI. *Cerebral Cortex, 7,* 181–192.
Fiez, J. A. (1996). Cerebellar contributions to cognition. *Neuron, 16,* 13–15.
Fisher, R. A., & Cornish, E. A. (1960). The percentile points of distributions having known cumulants. *Technometrics, 2,* 309–225.
Gao, J. H., Parsons, L. M., Bower, J. M., Xiong, J., Li, J., & Fox, P. T. (1996). Cerebellum implicated in sensory acquisition and discrimination rather than motor control. *Science, 272,* 545–547.
Gros, B. L., Blake, R., & Hiris, E. (1998). Anisotrophies in visual motion perception: a fresh look. *Journal of the Optical Society of America A, 15,* 2003–2011.
Grossberg, S., & Rudd, M. E. (1989). A neural architecture for visual motion perception: Group and element apparent motion. *Neural Networks, 2,* 421–450.
Howard, R. J., Brammer, M., Wright, I., Woodruff., P. W., Bullmore, E. T., & Zeki, S. (1996). A direct demonstration of functional specialization within motion-related visual and auditory cortex of the human brain. *Current Biology, 6,* 1015–1019.
Ivry, R. B., & Diener, H. C. (1991). Impaired velocity perception in patients with lesions of the cerebellum. *Journal of Cognitive Neuroscience, 3,* 355–366.
Johannson, G. (1973). Visual perception of biological motion and a model for its analysis. *Perception and Psychophysics, 14,* 201–211.
Lagae, L., Maes, H., Xiao, D.-K., Raiguel, S. E., & Orban, G. A. (1994). Responses of macaque STS neurons to optic flow components: A comparison of areas MT and MST. *Journal of Neurophysiology, 71,* 1596–1626.
Lappin, J. S., & Fuqua, M. A. (1983). Accurate visual measurement of three-dimensional moving patterns. *Science, 221,* 480–482.
McKee, S. P., & Welch, L. (1989). Is there a constancy for velocity? *Vision Research, 29,* 553–561.
Motter, B. C., Steinmetz, M. A., Duffy, C. J., & Mountcastle, V. B. (1987). Functional properties of parietal visual neurons: Mechanisms of directionality along a single axis. *Journal of Neuroscience, 7,* 154–176.
Nawrot, M., & Rizzo, M. (1995). Motion perception deficits from midline cerebellar lesions in humans. *Vision Research, 35,* 723–731.
Neri, P., Morrone, M. C., & Burr, D. C. (1998). Seeing biological motion. *Nature, 395,* 894–896.
Newsome, W. T. (1997). Deciding about motion: Linking perception to action. *Journal of Comparative Neurophysiology, A, 181,* 5–12.
Orban, G. A., De Wolf, J., & Maes, H. (1984). Factors influencing velocity coding in the human visual system. *Vision Research, 24,* 33–39.
Orban, G. A., Dupont, P., De Bruyn, B., Vogels, R., Vandenberghe, R., & Mortelmans, L. (1995). A motion area in human visual cortex. *Proceedings of the National Academy of Science, U.S.A., 92,* 993–997.
Pasternak, T., & Merigan, W. H. (1984). Effects of speed on direction discrimination. *Vision Research, 24,* 1349–1356.
Petersen, S. E., Fox, P. T., Posner, M. I., Mintun, M., & Raichle, M. E. (1989). Positron emission tomographic studies of the processing of single words. *Journal of Cognitive Neuroscience, 1,* 153–170.
Pollick, F. E., Fidopiastis, C. M., & Braden, V. (1999). Training the recognition of biological motion. *Investigative Ophthalmology and Visual Sciences, 40,* 3914.
Puce, A., Allison, T., Bentin S., Gore, J. C., & McCarthy, G. (1998). Temporal cortex activation in humans viewing eye and mouth movements. *Journal of Neuroscience, 18,* 2188–2199.
Oram, M. W., & Perrett, D. I. (1994). Responses of anterior superior temporal polysensory (STPa) neurons to ‘‘biological motion’’ stimuli. *Journal of Cognitive Neuroscience, 6,* 99–116.
Raymond, J. E. (1994). Directional anisotropy of motion sensitivity across the visual field. *Vision Research, 24,* 1029–1038.
Rogers, B. J., & Graham, M. (1979). Motion parallax as an independent cue for depth perception. *Perception, 8,* 125–134.
Saito, H., Yukie, M., Tanaka, K., Hikosaka, K., Fukada, Y., & Iwai, E. (1986). Integration of direction signals of image motion in the superior temporal sulcus of the macaque monkey. *Journal of Neuroscience, 6,* 145–157.
Schenk, T., & Zihl, J. (1997). Visual motion perception after brain damage: I. Deficits in global motion perception. *Neuropsychologia, 35,* 1289–1297.
Schenk, T., & Zihl, J. (1997). Visual motion perception after brain damage: II. Deficits in form-from-motion perception. *Neuropsychologia, 35,* 1299–1310.
Shadlen, M. N., Britten, K. H., Newsome, W. T., & Movshon, J. A. (1996). A computational analysis of the relationship be-

tween neuronal and behavioral responses to visual motion. *Journal of Neuroscience, 16,* 1486–1510.
Skudlarski, P., Constable, R. T., & Gore, J. C. (1999). ROC analysis of statistical methods used in functional MRI: Individual subjects. *Neuroimage, 9,* 311–329.
Sperling, G., Landy, M. S., Dosher, B. A., & Perkins, M. E. (1989). Kinetic depth effect and identification of shape. *Journal of Experimental Psychology: Human Perception and Performance, 15,* 116–125.
Sumi, S. (1984). Upside down presentation of the Johannson moving light spot pattern. *Perception, 13,* 283–286.
Sunaert, S., Van Hecke, P., Marchal, G., & Orban, G. A. (1999). Motion-responsive regions of the human brain. *Experimental Brain Research, 127,* 355–370.
Talairach, J., & Tournoux, P. (1988). *Co-planar stereotaxic atlas of the human brain*. New York: Thieme Medical.
Tittle, J. S., & Perotti, V. J. (1998). The perception of shape and curvedness from binocular stereopsis and structure from motion. *Perception and Psychophysics, 59,* 1167–1179.
Tootell, R. B. H., Hadjikhani, N. K., Mendola, J. D., Marrett, S., & Dale, A. M. (1998). From retinotopy to recognition: fMRI in human visual cortex. *Trends in Cognitive Sciences, 2,* 174–183.
Tootell, R. B. H., Reppas, J. B., Kwong, K. K., Malach, R., Born, R. T., Brady, T. J., Rosen, B. R., & Belliveau, J. W. (1995). Functional analysis of human MT and related visual cortical areas using magnetic resonance imaging. *Journal of Neuroscience, 15,* 3215–3230.
Vaina, L. M., Lemay, M., Bienfang, D. C., Choi , A. Y., & Nakayama, K. (1990). Intact ''biological motion'' and ''structure from motion'' perception in a patient with impaired motion mechanisms: A case study. *Visual Neuroscience, 5,* 353–369.
van de Grind, W. A., Koenderink, J. J., van Doorn, A. J., Milders, M. V., & Voerman, H. (1993). Inhomogeneity and anisotropies for motion detection in the monocular visual field of human observers. *Vision Research, 33,* 1089–1107.
Van Oostende, S., Sunaert S., Van Hecke, P., Marchal, G., & Orban G. A. (1997). The kinetic occipital (KO) region in man: An fMRI study. *Cerebral Cortex, 7,* 690–701.
Wallach, H., & O'Connell, D. N. (1953). The kinetic depth effect. *Journal of Experimental Psychology, 45,* 205–217.
Watanabe, T., Harner, A. M., Miyauchi, S., Saski, Y., Nielsen, M., Palomo, D., & Mukai, I. (1998). Task-dependent influences of attention on the activation of human primary visual cortex. *Proceedings of the National Academy of Science, U.S.A., 95,* 11489–11492.
Watson, J. D. G., Myers, R., Frackowiak, R. S. J., Hajnal, J. V., Woods, R. P., Mazziotta, J. C., Shipp, S., & Zeki, S. (1993). Area V5 of the human brain: Evidence from a combined study using positron emission tomography and magnetic resonance imaging. *Cerebral Cortex, 3,* 79–94.
Williams, D. W., & Sekuler, R. (1984). Coherent global motion percepts from stochastic local motion. *Vision Research, 24,* 55–62.
Xiao, D.-K., Marcar, V. L., Raiguel, S. E., & Orban, G. A. (1997). Selectivity of macaque MT/V5 neurons for surface orientation in depth specified by motion. *European Journal of Neuroscience, 9,* 956–964.